2009 American Control Conference
Hyatt Regency Riverfront, St. Louis, MO, USA
June 10-12, 2009

Sprung Mass Estimation for Off-Road Vehicles via Base-Excitation Suspension Dynamics and Recursive Least Squares

Benjamin L. Pence, Hosam K. Fathy, and Jeffrey L. Stein

Abstract—**This paper presents a novel method for identifying in real time the mass of an off-road vehicle using measurements of sprung and unsprung mass acceleration. The online estimate can be used for vehicle control strategies such as active safety control, traction control, and powertrain control. The online estimate is needed for vehicles whose mass varies significantly from one loading condition to another. Existing off-road mass estimation strategies that use suspension measurements typically require either known suspension force actuation or *a priori* knowledge of terrain characteristics.**

Our unique method for estimating online the mass of an off-road vehicle addresses existing limitations by applying base-excitation concepts to make the measured unsprung mass acceleration become a known input to the recursive least-squares estimator. We present computer simulations to demonstrate the method, and conclude that the method provides a practical solution for real-time, off-road vehicle mass estimation.

I. Introduction

This paper presents a novel method for online identification of off-road vehicle sprung mass. This estimate of sprung mass is to be used by online vehicle control systems including traction control, active safety control, and powertrain control systems. It is especially critical for vehicles whose mass varies greatly due to vast differences in cargo.

The literature contains many innovative papers and patents that address the problem of vehicle mass identification for on-road vehicles. Mostly, these techniques use longitudinal vehicle dynamics for mass identification. For discussion of these methods, see [1] and the references therein. Off-road terrain conditions, including the roughness of the terrain, rapidly changing road grade, reduced traction, and obstacles in the road unfortunately undermine many of the assumptions underlying these techniques and, therefore, add uncertainties that limit the effectiveness of these on-road techniques for use in off-road conditions.

While off-road terrain conditions limit the effectiveness of the longitudinal dynamics for mass identification, the vertical excitation they provide presents opportunities for identifying mass via suspension dynamics.

A few papers discuss ways to identify vehicle parameters including sprung mass using suspension dynamics.

Researchers have developed methods to identify the sprung mass when the input to the tire is specified by the user or is known prior to estimation, such as when a shaker table is used to simulate the ground input. Lin and Kortüm [2] used a four DOF model and a least squares method to identify vehicle mass, tire stiffness, and other unknown suspension parameters. Best and Gordon [3] integrated suspension dynamics equations to obtain impulse-momentum equations and used least-squares estimation to identify sprung mass. Shimp [4] derived a polynomial chaos expansion representation of a quarter-car model, and updated estimation parameters using the MIT rule.

Other researchers focused on estimating sprung mass from identifying the oscillations due to the free (or unforced) response of the vehicle. Tal and Elad [5] recommended using Fourier transforms to identify the natural frequency of vertical oscillations of the vehicle, then identified sprung mass from this knowledge and knowledge of the suspension spring stiffness constant.

Researchers have also exploited knowledge of suspension actuator forces in active or semi-active suspensions for sprung mass estimation. In [6], Rajamani *et al.* obtained an estimate of vehicle mass by using an adaptive observer to simultaneously obtain estimates of suspension states and parameters. Their method was for active suspensions in which a suspension force actuator provided a known forcing input. Ohsaku and Nakai [7] used a method in which they measured the pneumatic damping force. They used a least squares estimation method to identify sprung mass.

Finally, researchers have simultaneously estimated the ground input and vehicle mass using dual recursive least-squares [8].

This paper presents a novel base-excitation with recursive least-squares method that uses two acceleration signals plus the suspension spring force/displacement characteristic to estimate the sprung mass. The unsprung mass acceleration, instead of the ground displacement or suspension actuator, is treated as the system input. Thus the proposed method avoids the requirement of knowing or estimating the ground input, and no active suspension is required.

The remainder of the paper is formatted as follows: Section 2 discusses the solution formulation; Section 3 discusses the simulation set-up; Section 4 presents simulation results; Section 5 discusses simulation results, and Section 6 provides conclusions and recommendations.

Manuscript received September 22, 2008. This work was supported in part by the Automotive Research Center.

B. L. Pence is with the Department of Mechanical Engineering, University of Michigan, 2350 Hayward St., Ann Arbor, MI 48109 USA. (Phone: 734-936-5295; e-mail: bpence@umich.edu)

H. K. Fathy is with the Department of Mechanical Engineering, University of Michigan, 2350 Hayward St., Ann Arbor, MI 48109 USA. (e-mail: hfathy@umich.edu)

J. L. Stein is with the Department of Mechanical Engineering, University of Michigan, 2350 Hayward St., Ann Arbor, MI 48109 USA. (e-mail: stein@umich.edu)

978-1-4244-4524-0/09/$25.00 ©2009 AACC

II. SOLUTION FORMULATION

This section introduces the base-excitation model of the quarter-car suspension, discusses the filtering of base excitation measurements as an alternative to their integration, and presents the least-squares sprung mass and suspension damping estimation algorithm.

A. Quarter-car Base-excitation Model

A common approach to modeling the complex kinematics and dynamics of a quarter-car suspension system is to use the simplified two degree-of-freedom (DOF) system shown in Figure 1. Researchers (*e.g.* [9]) have analyzed the validity of this simplified model and offered analytical and experimental ways to identify the lumped parameters for this simplified system.

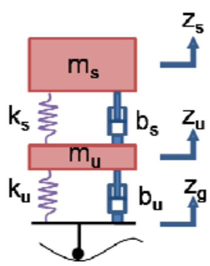

Fig. 1. 2-DOF Quarter-Car Suspension Model.

Using the full 2 DOF model for sprung mass estimation requires knowledge of the ground input z_g. Instead, the proposed method uses a base-excitation suspension model which treats the (measured) unsprung mass acceleration as the system input. It is developed as follows. Consider a free body diagram (see Figure 2) of the sprung mass from the system shown in Figure 1. The system equations follow from the free body diagram:

$$m_s(\ddot{z}_s - \ddot{z}_u + \ddot{z}_u) + b_s(\dot{z}_s - \dot{z}_u) + k_s(z_s - z_u) = 0 \quad (1)$$

Letting $x = z_s - z_u$, and moving the last $\ddot{z}_u$ term to the right-hand side, the equation becomes as follows:

$$m_s\ddot{x} + b_s\dot{x} + k_s x = -m_s\ddot{z}_u \quad (2)$$

The unsprung mass acceleration $\ddot{z}_u$ can be viewed as the input to the system.

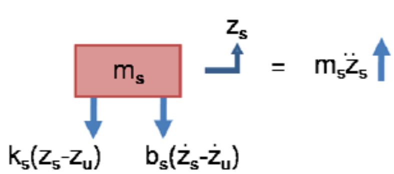

Fig. 2. Sprung Mass Free Body Diagram

B. Filtering of Acceleration Signals

We would like to be able to use only sprung and unsprung acceleration signals for mass identification. Equation 1, however, is also a function of suspension displacement and velocity. In the absence of noise we could simply integrate the acceleration signals to obtain displacement and velocity, however, even a small amount of signal noise causes the integration to quickly drift. An alternative to directly integrating the acceleration signals is to use filtering:

$$m_s\left\{\frac{s^2}{\Lambda(s)}\right\}\ddot{z}_s + b_s\left\{\frac{s}{\Lambda(s)}\right\}(\ddot{z}_s - \ddot{z}_u) + k_s\left\{\frac{1}{\Lambda(s)}\right\}(\ddot{z}_s - \ddot{z}_u) = 0 \quad (3)$$

where $\left\{\frac{s^2}{\Lambda(s)}\right\}f(t)$ represents a time domain signal $f(t)$ filtered by the Laplace domain filter $\left\{\frac{s^2}{\Lambda(s)}\right\}$, and $\Lambda(s)$ is a polynomial in s such that the filter $\left\{\frac{s^2}{\Lambda(s)}\right\}$ is causal: e.g. $\Lambda(s) = s^2 + 2\zeta\omega_n s + \omega_n^2$ where ζ and ω_n are the filter damping ratio and natural frequency. Equation 3 is no longer a function of suspension displacement and velocity. Rewriting Equation 3 in a form that is more suited for parameter estimation gives the following:

$$-k_s\left\{\frac{1}{\Lambda(s)}\right\}(\ddot{z}_s - \ddot{z}_u) = [m_s \quad b_s]\begin{bmatrix}\left\{\frac{s^2}{\Lambda(s)}\right\}\ddot{z}_s \\ \left\{\frac{s}{\Lambda(s)}\right\}(\ddot{z}_s - \ddot{z}_u)\end{bmatrix} \quad (4)$$

For brevity, Equation 4 will be written as:

$$y = \theta^T\phi \quad (5)$$

C. Recursive Least-Squares Estimation

We simultaneously estimate the vehicle sprung mass and suspension damping coefficient using recursive least-squares estimation. The recursive least squares estimate is calculated by [11]

$$\dot{\hat{\theta}} = P(y - \hat{\theta}^T\phi)\phi \quad (6)$$

$$\dot{P} = -P\frac{\phi\phi^T}{1+\phi^T P\phi}P, \quad (7)$$

where P is a 2 by 2 symmetric covariance matrix and $\hat{\theta}$ is the least-squares estimate of θ. Both P and $\hat{\theta}$ require initialization (see [11]). The vectors y, θ, and ϕ were defined in Equations 4 and 5, and $\hat{\theta}$ is an estimate of the unknown parameter vector θ.

III. SIMULATION SETUP

A. Simulation Parameters

This paper presents simulations of the quarter-car system (see Figure 1) using parameter data from an analysis of a HMMWV vehicle (see [10]). The values used in the simulation are shown in Table 1. The suspension damping force with respect to velocity was piece-wise linear. Other system components were modeled as linear.

TABLE I
QUARTER-CAR SIMULATION AND MODEL PARAMETERS

Symbol	Description	Value
Ts	Sampling Period	0.005 s
m_s	Vehicle sprung mass	803 kg
k_s	Suspension spring stiffness	63,528 N/m
$b_{s,ext}$	Damping coefficient for extension	3,428 N-s/m
$b_{s,cmp}$	Damping coefficient for compression	10,571 N-s/m
$\zeta_{s,ext}$	Damping ratio for extension	0.24
$\zeta_{s,cmp}$	Damping ratio for compression	0.74
m_u	Vehicle unsprung mass	98 kg
k_u	Tire stiffness coefficient	204,394 N/m
b_u	Tire damping coefficient	0 N-s/m
$P(0)$	Initial estimator covariance matrix	$\begin{bmatrix} 1000 & 0 \\ 0 & 1000 \end{bmatrix}$
$\theta^T(0)$	Transpose of the initial estimate vector	$[0 \quad 0]$

All units are SI: "s" indicates second; "kg" indicates kilogram; "N" indicates Newton; and "m" indicates meter.

B. The Terrain Model

This work used an autoregressive integrated moving average ARIMA(8,1,0) model to simulate an off-road terrain profile and to provide a vertical ground input z_g to the quarter-car simulation. Kern suggested this type of terrain model and gave example ARIMA(8,1,0) coefficients [12]. A plot of the resulting terrain profile is shown in Figure 3.

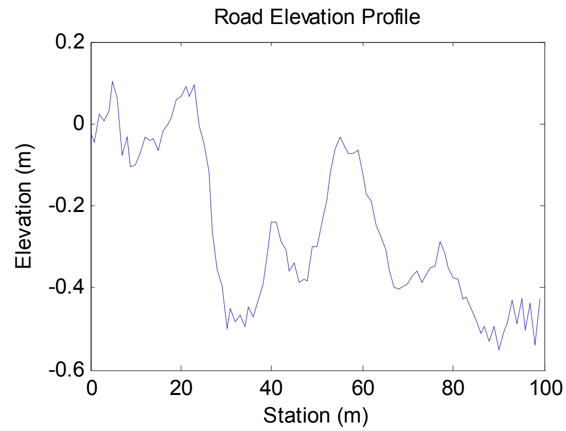

Fig. 3. Sample Realization of ARIMA Terrain Profile

IV. SIMULATION RESULTS

This paper presents simulation results to demonstrate the effect of varying a number of simulation parameters including the effect of suspension nonlinearities, sensor noise, filter tuning, and vehicle speed. Unless otherwise specified, the values for these parameters are as shown in Tables 1 and 2.

TABLE II
NOMINAL VALUES FOR SIMULATION VARIABLES

Symbol	Description	Value Unless Specified Below
Vel	Vehicle speed	8 m/s
$\Lambda(s)$	Filter denominator	$s^2 + 2\zeta\omega_n s + \omega_n^2$
ω_n	Filter natural frequency	6 rad/s
ζ	Filter damping ratio	0.1
SNR	Signal-to-noise ratio	25 dB
σ_w	Gaussian white noise standard deviation	0.37 m/s^2

The simulation results are illustrated in Figures 4 through 8. Figure 4 shows the convergence of the proposed method for four cases:

1. No signal noise and no suspension nonlinearities.
2. Additive Gaussian white signal noise with standard deviation of 0.37 m/s^2 (25 dB signal-to-noise ratio) and no suspension nonlinearities.
3. No signal noise but with piecewise linear suspension damping with a damping ratio of 0.24 for extension and 0.74 for compression.
4. Both signal noise with standard deviation 0.37 m/s^2 and piecewise linear suspension damping with a damping ratio of 0.24 for extension and 0.74 for compression.

Numerical values corresponding to Figure 4 are given in Table 3.

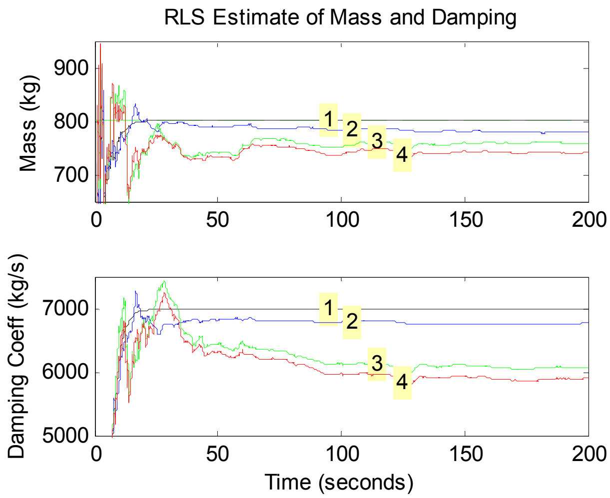

Fig. 4. Impact of Sensor Noise and Suspension Damper Nonlinearity on Estimator Performance

TABLE III
SIMULATION RESULTS CORRESPONDING TO FIGURE 4

Run	Mass (kg)	Error (%)	Damping (N-s/m)
1	803	0%	7000
2	781	2.7%	6773
3	759	5.4%	6075
4	742	7.6%	5902

Note: The true sprung mass was 803 kg. For the linear runs (1 and 2), the true Damping was 7000 N-s/m. For runs 3 and 4, the damping was piecewise linear. Estimation errors are computed based on mass estimates after 200 seconds.

Figure 5 shows simulation results for varying the filter natural frequency ω_n from 1 to 20 rad/s. The five cases shown are as follows:

1. $\omega_n = 1$ radians per second
2. $\omega_n = 3$ radians per second
3. $\omega_n = 6$ radians per second
4. $\omega_n = 10$ radians per second
5. $\omega_n = 20$ radians per second

As seen in the figure, if ω_n is too low (signal 1), then the estimate tends to drift. When ω_n is too high (signal 5), the estimate becomes less accurate. For the given simulations, the estimate was most accurate for ω_n in the range of 3 to 10 rad/s. These values correspond to signals 2-4 in Figure 5. Table 4 summarizes the simulation results for varying ω_n.

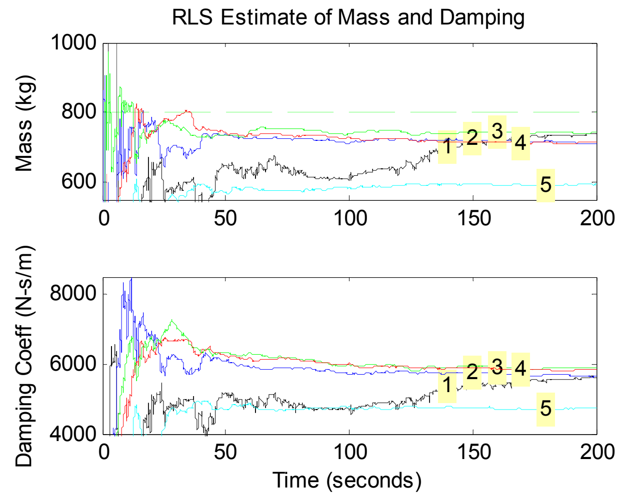

Fig. 5: Results of varying the filter natural frequency ω_n.

TABLE IV
SIMULATION RESULTS FOR VARYING ω_n

ω_n	Mass (kg)	Error (%)	Damping (N-s/m)
1	737	8.2%	5602
3	710	11.5%	5634
6	741	7.6%	5902
10	713	11.1%	5839
20	594	26%	4734

Note: The true sprung mass was 803 kg. Estimation errors are based on estimates after 200 seconds.

In Figure 6, the damping ratio ζ of the filter $\Lambda(s)$ was varied between 0.01 and 0.5. The five signals shown are for

1. $\zeta = 0.01$
2. $\zeta = 0.05$
3. $\zeta = 0.1$
4. $\zeta = 0.25$
5. $\zeta = 0.5$

Table 5 summarizes the results for varying ζ.

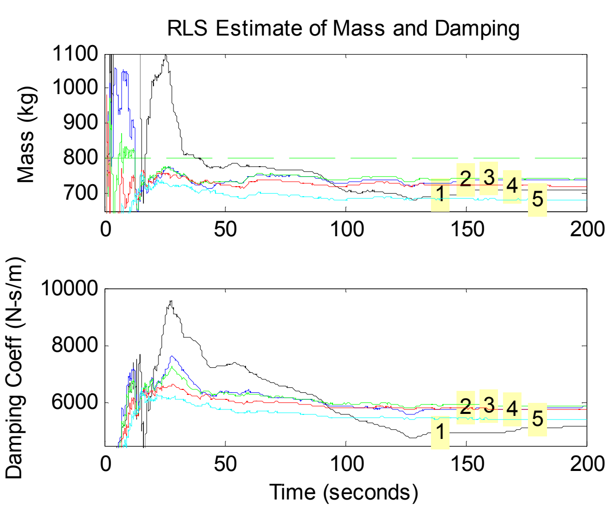

Fig. 6: Results for varying the damping ratio ζ from 0.01 to 0.5.

TABLE V

SIMULATION RESULTS FOR VARYING ζ

ζ	Mass (kg)	Error (%)	Damping (N-s/m)
0.01	709	11.8%	5173
0.05	740	7.9%	5846
0.1	741	7.6%	5902
0.25	720	10.4%	5737
0.5	680	15.3%	5394

The true sprung mass was 803 kg. Errors correspond to estimates at 200 seconds.

Figure 7 shows the effect of varying the vehicle speed between 2 m/s (4.5 mph) and 16 m/s (36 mph). The five results displayed are for

1. 2 meters per second
2. 4 meters per second
3. 8 meters per second
4. 12 meters per second
5. 16 meters per second

For speeds of 8 meters per second and above, the excitation to the tire was large enough to cause the tire to leave the ground. For 8 m/s, the tire was off ground for 0.05% of the time. For 12 m/s, the tire was off ground for 0.78% of the time, and for 16 m/s, the tire was off ground for 4.45% of the time.

Table 6 summarizes the results for different longitudinal vehicle speeds.

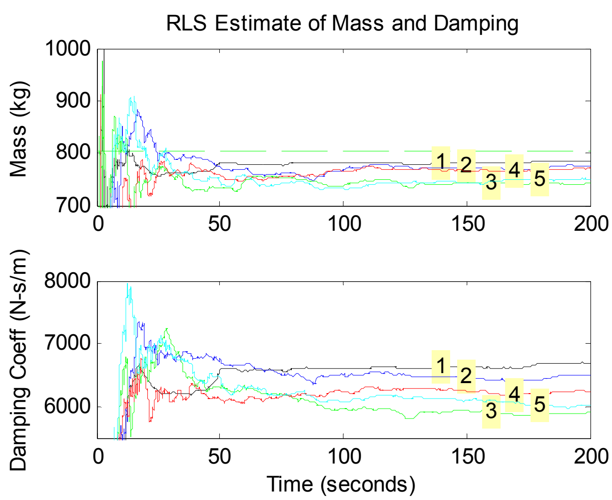

Fig. 7. Effect of Vehicle Speed on Estimator Performance

TABLE VI

SIMULATION RESULTS FOR VARYING VEHICLE SPEED

Vehicle Speed	Mass (kg)	Error (%)	Damping (N-s/m)
2 m/s	786	2.2%	6697
4 m/s	775	6.5%	6493
8 m/s	741	7.6%	5900
12 m/s	770	4.1%	6241
16 m/s	750	6.6%	6011

The true sprung mass was 803 kg. Errors correspond to estimates at 200 seconds.

Figure 8 and Table 7 show the effect of varying the amount of additive Gaussian white noise on the convergence of the proposed method. The signals used for estimation were the acceleration signals of the sprung and unsprung masses. The signal-to-noise ratio (SNR) in decibels was calculated by the following equation:

$$RMS(dB) = 20log_{10}\left(\frac{RMS\ signal}{RMS\ noise}\right) = 20log_{10}\left(\frac{\sigma_{signal}}{\sigma_{noise}}\right)$$

where σ_{signal} is the sample standard deviation of the signal, and σ_{noise} is the standard deviation of the noise. The second equality holds when both the signal and noise are zero mean.

We ran simulations for signal-to-noise ratios between infinite (no noise) and 15 dB. The five runs displayed are as follows:

1. No noise
2. 30 decibels signal-to-noise ratio
3. 25 decibels signal-to-noise ratio
4. 20 decibels signal-to-noise ratio
5. 15 decibels signal-to-noise ratio

Figure 8 shows that as the amount of noise increased, the accuracy decreased.

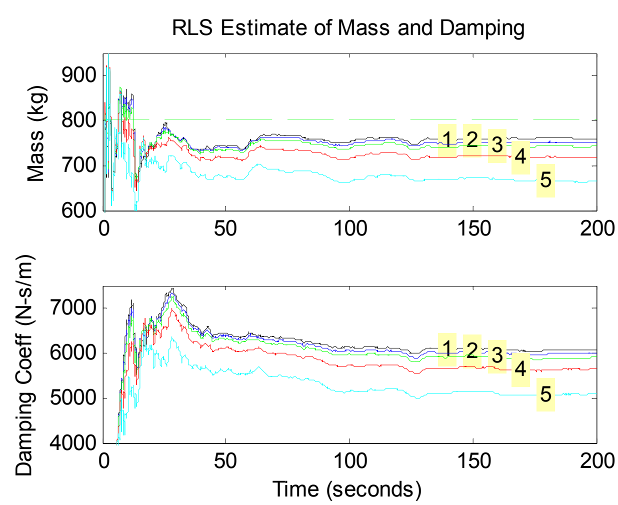

Fig. 8. Impact of Sensor Noise on Estimator Performance

TABLE VII
SIMULATION RESULTS CORRESPONDING TO FIGURE 8

SNR*	Mass (kg)	Error (%)	Damping (N-s/m)
Infinite	759	5.4%	6075
30 dB	751	6.5%	5990
25 dB	741	7.6%	5902
20 dB	718	10.6%	5653
15 dB	665	17.2%	5100

*Signal-to-noise ratio. The true sprung mass was 803 kg. Errors correspond to estimates at 200s.

V. DISCUSSION OF RESULTS

For a typical case, such as Run 4 of Figure 4 and Table 3, the estimate of vehicle mass converged to within 8% of the true value in less than 100 seconds.

An important point to note from Figure 4 is that for the linear suspension model with noiseless signals (signal marked "1"), the proposed method converged to the exact values of sprung mass and suspension damping illustrating the fact that the filtering method of Equation 3 is an exact equation. Thus by filtering, we were indeed able to remove the need of directly measuring the suspension velocity and displacement signals.

The proposed method was sensitive to tuning the filter $\Lambda(s)$ parameters ζ and ω_n. Filtering eliminates the need for integrating the acceleration measurements to obtain suspension velocity and displacement signals. Lower values of ω_n and ζ cause the filter to respond like an integrator/double integrator over a broader range of frequencies. However, if the values of ω_n and ζ are chosen to be too low, they cause the filtered signals to drift resulting in inaccurate estimates. Such cases are illustrated by Run 5 in Figures 5 and 6 and Tables 4 and 5. A good range for ω_n was found to be between 3 and 10 radians per second, and a good range for ζ was found to be between 0.05 and 0.25.

Finally, the sprung mass estimate degrades almost proportionally to the amount of sensor noise as seen in Figure 8 and Table 7.

VI. CONCLUSIONS

This paper has introduced a novel method of estimating vehicle mass using only sprung and unsprung mass acceleration signals and has demonstrated its effectiveness via simulation. The method required no *a priori* knowledge of ground input and no suspension force actuator. The method was derived from a base-excitation model of a quarter-car suspension, making the unsprung mass acceleration a measured system input. Estimates of suspension velocity and displacement were obtained via filtering. A second order, recursive, least-squares estimator was used to simultaneously estimate vehicle sprung mass and (average) damping coefficient. The sprung mass estimates typically converged to within 8% of the true value in less than 100 seconds.

The proposed method was sensitive to filter parameters and signal noise. However, simulation results suggest that the proposed estimator may prove viable for practical sprung mass estimation in off-road vehicles using inexpensive instrumentation. Ongoing work considers using a recursive total least squares estimator, which accounts for both regressor and signal noise, and is therefore expected to perform better than the least squares method. Also, ongoing work is directed towards further validation of the proposed estimator using higher-fidelity validation models and experimental data.

REFERENCES

[1] H. K. Fathy, D. Kang, J.L. Stein, "Online Vehicle Mass Estimation Using Recursive Least Squares and Supervisory Data Extraction" 2008 American Control Conference, Seattle, WA, USA

[2] Y. Lin and W. Kortüm "Identification of system physical parameters for vehicle systems with nonlinear components" 1992, *Vehicle System Dynamics*, 20:6, 354 — 365

[3] M. C. Best and T. J. Gordon, "Suspension System Identification Based on Impulse-Momentum Equations" 1998, *Vehicle System Dynamics* Supplement 28, pp 598-618

[4] S. Shimp III. "Vehicle Sprung Mass Parameter Estimation Using an Adaptive Polynomial-Chaos Method", 2008, Master's Thesis, Virginia Tech.

[5] R. Tal and S. Elad, "Method for determining weight of a vehicle in motion", 1999, U.S. Patent No. 5,973,273

[6] R. Rajamani and J. K. Hedrick, "Adaptive Observers for Active Automotive Suspensions: Theory and Experiment", 1995, IEEE Transactions on Control Systems Technology, Vol. 3. No. 1, March 1995

[7] S. Ohsaku and H. Nakai, "Sprung Mass Estimating Apparatus" 2000, U.S. Patent No. 6,055,471

[8] K. Huh, S. Lim, J. Jung, D. Hong, S. Han, K. Han, H. Y. Jo, J. M. Jin "Vehicle Mass Estimator for Adaptive Roll Stability Control", 2007, SAE paper 2007-01-0820.

[9] C. Kim and P. I. Ro, "Reduced-order modelling and parameter estimation for a quarter-car suspension system", 2000 Proc. Instn Mech Engrs Vol 214 Part D

[10] Z. Lou, C. B . Winkler, R. D. Ervin, F. E. Filisko, P. J. Th. Venhovens, G. E. Johnson, "Electrorheology for Smart Automotive Suspensions" June 1994, UMTRI-94-15 pg.23-24

[11] P. A. Ioannou and J. Sun, "Adaptive Robust Adaptive Control", 1996 Prentice-Hall, Inc. pg. 223

[12] J. V. Kern, "The Development of Measurement and Characterization Techniques of Road Profiles", 2007, Master's Thesis, Virginia Polytechnic Institute and State University